Optica Applicata, Vol. XXVI, No. 3, 1996

Estimation of the efficiency of harmonic generation in nonlinear crystals with 1064 nm Gaussian laser pulses

R. DABU, C. FENIC, A. STRATAN

Institute of Atomic Physics, Laser Department, P.O. Box MG 6, Bucharest, Romania.

L. MUSCALU

Prooptica, Bucovina Street 4, 74404 Bucharest, Romania.

We analyse optical parameters related to the generation of the harmonics of Nd:YAG laser radiation in different nonlinear crystals (KTP, LBO, KDP, ADP). In the case of non-focused Gaussian laser pulses, under the depleted pump assumption, simple formulae for the calculus of the second harmonic generation (SHG) efficiency are deduced. The experimentally measured angular acceptance width and SHG efficiency are compared with the theoretically calculated values.

1. Introduction

The efficiency of frequency converting lasers has increased in the last years as a result of the development of new nonlinear crystals (KTP, LBO, BBO, Mg:$LiNbO_3$) [1]–[4]. The conversion efficiency of Nd:YAG laser fundamental radiation (1064 nm) to a harmonic is determined by the characteristics of the incident beam (temporal and spatial power distribution, divergence, line bandwidth) and the optical properties of the nonlinear crystal (nonlinear effective coefficient, angular acceptance, spectral acceptance, thermal acceptance, walk-off angle, damage threshold, optical quality, transparency).

The power conversion efficiency to second harmonic (SH) of a fundamental plane wave propagating in a nonlinear medium was calculated in [5], [6]. A comparative theory of walk-off limited type II versus type I SHG with Gaussian beams, under the undepleted pump assumption, was developed in [7].

The aim of this paper is to establish analytical expressions for the phase matching parameters involved in harmonic generation, and to deduce simple formulae for the evaluation of the SHG efficiency in nonlinear crystals with non-focused Gaussian beams, under the depleted pump conditions.

2. Theory

An efficient harmonic generation in a nonlinear crystal is possible for a certain propagation direction in which three electromagnetic waves may simultaneously

satisfy the matching relations for frequency and wave vector

$$\omega_3 = \omega_1 + \omega_2,$$
$$\mathbf{k}_3 = \mathbf{k}_1 + \mathbf{k}_2. \tag{1}$$

For SHG, $\omega_1 = \omega_2 = \omega$, $\omega_3 = 2\omega$.

For a collinear interaction, the phase matching condition is

$$\Delta k = k_3 - k_2 - k_1 = \frac{1}{c}[\omega_3 n_3(\theta,\varphi,T) - \omega_2 n_2(\theta,\varphi,T) - \omega_1 n_1(\theta,\varphi,T)] = 0 \tag{2}$$

where n_i ($i = 1, 2, 3$) is the refractive index, T is the temperature, c is the light speed, θ is the angle from the crystal z-axis, φ is the angle between the x-axis and plane of the z-axis and the propagation direction. The phase matching condition for collinear SHG is

$$2n_3 = n_1 + n_2. \tag{3}$$

The critical phase matching (CPM) is accomplished at $(\theta,\varphi) \neq 0°$ or 90° [6]. The phase mismatch Δk depends linearly on tuning angles, $\Delta k \sim \delta\theta, \delta\varphi$.

There is a noncritical phase matching (NCPM) if the phase matching direction is along one of the crystallographic axes [6]. Δk depends on much smaller quadratic terms $(\delta\theta)^2$, $(\delta\varphi)^2$. The angular acceptance is very large, there are no walk-off effects owing to the double refraction. There is NCPM for the angle θ if the phase matching direction is in the xy crystallographic plane, and for the angle φ if the phase matching direction is in the xz or yz plane.

For CPM the angular acceptance is $A_a = l_c \Delta\alpha$, where l_c is the crystal length, and $\Delta\alpha$ is the full width at half maximum (FWHM) external angular tuning range (the acceptance angle over which the crystal can be tilted before the harmonic power decreases to less than half). For NCPM the angular acceptance is $l_c^{1/2}\Delta\alpha$. The spectral acceptance is $A_s = l_c \Delta\lambda$, where $\Delta\lambda$ is the FWHM spectral bandwidth of the crystal. The thermal acceptance is $A_t = l_c \Delta T$, where ΔT is the FWHM temperature bandwidth of the crystal. The walk-off angle ρ between the direction of the power flow of fundamental and harmonic waves is determined by the crystal birefringence.

In the case of incident laser pulses with Gaussian temporal and spatial profile, it is essential to evaluate the SHG conversion efficiency of the peak irradiance (power density) and of the energy. The conversion efficiency of peak irradiance η_{gp}, defined as the ratio of SH peak irradiance $I_m(2\omega)$ to fundamental peak irradiance I_m, for exact phase matching ($\Delta k = 0$), in the near field region ($l_c \ll b/2$, where b is the confocal parameter), is given by (see Appendix)

$$\eta_{gp} = \tanh^2 [l_g(\zeta I_m)^{1/2}] \tag{4}$$

where l_g is the interaction length of incident and SH beams

$$l_g = l_w \operatorname{erf}\left(\frac{\sqrt{\pi} l_c}{2 l_w}\right) \tag{5}$$

where l_w is the walk-off length (see Appendix)

$$I_m = \frac{1.88 W_\omega}{\pi \tau w_1^2} \tag{6}$$

where W_ω, τ and w_1 are the energy, FWHM pulse width, and $1/e^2$ radius of the incident beam, respectively.

The nonlinear coupling parameter ζ is given by [5], [6], [8]

$$\zeta = \frac{8\pi^2 d_{eff}^2 g_\alpha g_\lambda}{n_1 n_2 n_3 \varepsilon_0 c \lambda^2} \tag{7}$$

where d_{eff} is the nonlinear effective coefficient of the crystal, ε_0 is the permittivity of vacuum, λ is the fundamental wavelength (1064 nm), g_λ and g_α are the reduction coefficients owing to the limited phase matching spectral bandwidth and angular acceptance width of the nonlinear crystal. If the laser line-shape and the spectral acceptance functions are approximated by Gaussians, g_λ is given by [8]

$$g_\lambda = \frac{\int_{-\infty}^{\infty} f(\Delta\lambda_f) h(\Delta\lambda) d\lambda}{\int_{-\infty}^{\infty} f(\Delta\lambda_f) d\lambda} \simeq \left[\frac{(\Delta\lambda)^2}{(\Delta\lambda)^2 + (\Delta\lambda_f)^2}\right]^{1/2} \tag{8}$$

where $f(\Delta\lambda_f)$ is the intensity spectral line-shape function of the fundamental beam with FWHM $\Delta\lambda_f$, $h(\Delta\lambda)$ is the spectral acceptance function with FWHM $\Delta\lambda$ bandwidth. If one uses the same approximation for the angular acceptance function, g_α is given by

$$g_\alpha \simeq \left[\frac{(\Delta\alpha)^2}{(\Delta\alpha)^2 + (\Delta\alpha_f)^2}\right]^{1/2} \tag{9}$$

where $\Delta\alpha_f$ is the full divergence angle of the fundamental TEM_{00} beam.

The small-signal conversion efficiency of the peak irradiance ($\eta_{gp} \ll 1$) is given by

$$\eta_{gp} = \frac{1.88 l_g^2 \zeta W_\omega}{\pi \tau w_1^2}. \tag{10}$$

At NCPM ($\rho = 0$) or very small walk-off angle ($l_c \ll l_w$, $l_g \simeq l_c$), neglecting the diffraction ($w_1 < r_0$, where r_0 is the radius of the input aperture of the nonlinear crystal), the energy conversion efficiency (ECE) η_{ge} for a Gaussian laser pulse can be estimated by

$$\eta_{ge} = \frac{W_{2\omega}}{W_\omega} \simeq \frac{3.76}{\tau w_1^2} \int_{t=-\infty}^{\infty} \int_{r=0}^{r_0} \exp\left[-\frac{2r^2}{w_1^2} - \frac{t^2}{(0.6\tau)^2}\right] \tanh^2\left[l_c \sqrt{\zeta I_m} \exp\left[-\frac{r^2}{w_1^2} - \frac{t}{2(0.6\tau)^2}\right]\right] r dr dt \tag{11}$$

where $W_{2\omega}$ is the SH energy.

The small-signal ECE, with Δk wave vector mismatch, and negligible walk-off angle is

$$\eta_{ge} \simeq \frac{0.66 l_c^2 \zeta W_\omega}{\pi \tau w_1^2} \frac{\sin^2(\Delta k l_c/2)}{(\Delta k l_c/2)^2}. \tag{12}$$

The sinc^2 function is reduced to 1/2 when $\Delta k \simeq \frac{0.886\pi}{l_c}$.

The KTP is a biaxial crystal with a high nonlinear effective coefficient $d_{eff}(\text{KTP}) \simeq 8.3 d_{36}(\text{KDP}) \simeq$ 3.18 pm/V, and a large angular acceptance for SHG [9], [10]. In a KTP crystal, type II cut ($oe \rightarrow e$) for SHG at 1064 nm, $\theta = 90°$, the phase matching condition is

$$2n_{xy,\varphi}^{2\omega} = n_{xy,\varphi}^{\omega} + n_z^{\omega} \tag{13}$$

with the refractive index $n_{xy,\varphi}^{\omega}$ for the fundamental wave propagation in the xy crystallographic plane being given by

$$n_{xy,\varphi}^{\omega} = \frac{n_x^{\omega} n_y^{\omega}}{[(n_x^{\omega})^2 \cos^2\varphi + (n_y^{\omega})^2 \sin^2\varphi]^{1/2}} \tag{14}$$

where n_x, n_y, n_z are the refractive indexes for linear polarization along x,y,z crystallographic axes. It follows from (13) that $\varphi \simeq 23.5°$.

To calculate the angular acceptance, spectral acceptance, and thermal acceptance one expands the phase mismatch Δk near the exact phase matching angle α_0 ($\alpha = \varphi, \theta$), wavelength λ_0, and temperature T_0, respectively

$$\Delta k(\alpha) = \Delta k\Big|_{\alpha=\alpha_0} + \frac{\partial \Delta k}{\partial \alpha}\Big|_{\alpha=\alpha_0} (\Delta\alpha) + \frac{1}{2}\frac{\partial^2 \Delta k}{\partial \alpha^2}\Big|_{\alpha=\alpha_0} (\Delta\alpha)^2,$$

$$\Delta k(\lambda) = \Delta k\Big|_{\lambda=\lambda_0} + \frac{\partial \Delta k}{\partial \lambda}\Big|_{\lambda=\lambda_0} (\Delta\lambda),$$

$$\Delta k(T) = \Delta k\Big|_{T=T_0} + \frac{\partial \Delta k}{\partial T}\Big|_{T=T_0} (\Delta T). \tag{15}$$

The optical properties of a KTP II crystal can be calculated using the following expressions [5], [14]:

$$l_c \Delta\varphi_{\text{KTP}} = n_{xy,\varphi}^{\omega} \frac{0.886\lambda}{\sin 2\varphi \left\{ (n_{xy,\varphi}^{2\omega})^3 \left[\frac{1}{(n_x^{2\omega})^2} - \frac{1}{(n_y^{2\omega})^2} \right] - \frac{1}{2}(n_{xy,\varphi}^{\omega})^3 \left[\frac{1}{(n_x^{\omega})^2} - \frac{1}{(n_y^{\omega})^2} \right] \right\}},$$

$$\sqrt{l_c}\,\Delta\theta_{\text{KTP}} = \frac{2 n_{xy,\varphi}^{\omega} \sqrt{0.886\lambda}}{\left\{ (n_z^{\omega})^3 \left[\frac{1}{(n_{\theta,\varphi}^{\omega})^2} - \frac{1}{(n_z^{\omega})} \right] \right\}^{1/2}},$$

$$l_c \Delta\lambda_{KTP} = \frac{0.886\lambda}{\left[\left(\frac{\partial n_{xy,\varphi}}{\partial\lambda}\right)_{\lambda/2} - \left(\frac{\partial n_{xy,\varphi}}{\partial\lambda}\right)_{\lambda} - \left(\frac{\partial n_z}{\partial\lambda}\right)_{\lambda}\right]},$$

$$l_c \Delta T_{KTP} = \frac{0.886\lambda}{\left[\frac{2\partial n^{2\omega}_{yx,\varphi}}{\partial T} - \frac{\partial n^{\omega}_{xy,\varphi}}{\partial T} - \frac{\partial n^{\omega}_{z}}{\partial T}\right]},$$

$$\rho_{1,2KTP} = \arctan\frac{[(n_y^{\omega,2\omega}/n_x^{\omega,2\omega})^2 - 1]\tan\varphi}{1 + [n_y^{\omega,2\omega}/n_x^{\omega,2\omega}]^2\tan^2\varphi} \tag{16}$$

where

$$n_{\theta,\varphi} = \left[\frac{\cos^2\varphi}{n_x^2} + \frac{\sin^2\varphi}{n_y^2}\right]^{-1/2} \tag{17}$$

is the refractive index along the phase matching direction, ρ_1 is the Poynting vector walk-off angle of the *e*-polarized fundamental beam, ρ_2 is the walk-off angle of the *e*-polarized SH beam.

LBO is a biaxial moderately nonlinear harmonic generating crystal [d_{eff}(LBO) $\simeq 2.2 d_{36}$(KDP)] with low angular sensitivity for SHG and third harmonic generation (THG) at 1064 nm [1], [4]. In an LBO doubler at 1064 nm, cut for type I ($oo \rightarrow e$) phase matching, $\theta = 90°$, the relation between the refractive index of the interacting waves is $n^{2\omega}_{xy,\varphi} = n^{\omega}_z$. It results that $\varphi \simeq 10.8°$.

KDP and ADP are uniaxial crystals ($n_x = n_y$) with relatively low nonlinear coefficients [d_{36}(ADP) $\simeq 1.2 d_{36}$(KDP)] [6]. The KDP tripler and the ADP quadrupler at 1064 nm are cut for type I ($oo \rightarrow e$) phase matching with $\theta = 47°$, $\varphi = 45°$, and $\theta = 80°$, $\varphi = 45°$, respectively. The analytical expressions of the optical properties of LBO I, KDP I, and ADP I crystals are deduced in the same manner as for KTP II crystal. The calculated values of the optical properties of the nonlinear crystals mentioned above are summarized in Table 1. We used the Sellmeier equations and therm-optic coefficients given in [4], [11], [12] and Data Sheets from Castech Fujian China and Eksma Lithuania.

Table 1. Calculated optical properties of different nonlinear crystals

	CPM A_a [cm × mrad]	NCPM A_a [cm$^{1/2}$ × mrad]	A_s [cm × nm]	A_t [cm × K]	ρ [mrad]
KTP II doubler	16.4	76	0.62	28	$\rho_1 = 3$, $\rho_2 = 4.4$
LBO I doubler	7.2	76.6	3.7	10.9	6.4
KDP I tripler	1.04		1.09	8.03	30
ADP I quadrupler	2.08		0.2	2.9	11.3

3. Experimental set-up

The experimental arrangement is presented in Figure 1. The dynamic stable resonator of the Nd:YAG laser oscillator is 1.35 m long, having a high reflecting flat-convex mirror M_1 with curvature radius $R_1 = 4.7$ m, and an output concave mirror M_2 with radius $R_2 = 2.48$ m. The output mirror is provided with a second curvature to get a beam leaving the resonator with a plane phase front [13]. The

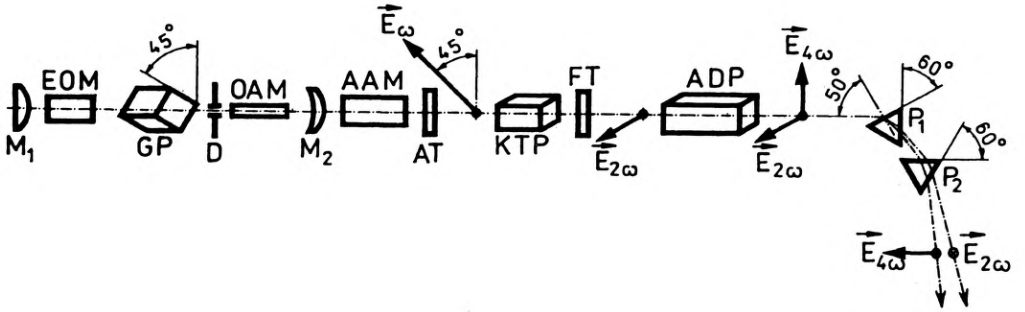

Fig. 1. Schematic diagram showing the experimental set-up for the SHG in KTP II crystal and the fourth harmonic generation (4HG) in ADP I crystal

electrooptic Q-switch is obtained with the longitudinal electrooptic modulator (EOM) and Glan prism (GP). The diameter of the aperture D for TEM_{00} selection is 2.6 mm. The active media OAM and AAM of the laser oscillator and of the amplifier are Nd:YAG rods, 75 mm length, 3 mm diameter and 80 mm length, 6 mm diameter, respectively. Both rods are pumped in close-coupled pump cavities with Spectralon diffuse reflectors. The laser output energy is attenuated with a set of calibration attenuators (AT). The SH is separated from fundamental beam with a BG18 glass filter (FT) transparent at 532 nm and opaque at 1064 nm.

We used in our SHG experiments a KTP II crystal, $4 \times 4 \times 5$ mm^3 size, made by Castech Fujian China and a LBO I crystal, $4 \times 4 \times 12$ mm^3 size, made by Eksma Lithuania. Both crystals were AR coated at 1064 and 532 nm. They were fastened to mechanical mounts equipped with micrometric screws for fine rotation around three orthogonal axes. The LBO crystal was irradiated through a beam compressor which reduces the diameter of the incident beam, $w_{1_{LBO}} = w_{1_{KTP}}/2$. The y,z crystallographic axes of the KTP were oriented at 45° angle from the electric field vector $\mathbf{E}_\omega$ of the incident wave. The polarization direction of the electric field $\mathbf{E}_{2\omega}$ of the SH was oriented at 45° angle from $\mathbf{E}_\omega$ and lay in the xy crystallographic plane of KTP crystal. In the case of LBO I doubler, z crystallographic axis was parallel with $\mathbf{E}_\omega$ and perpendicular to $\mathbf{E}_{2\omega}$. The angular tuning of KTP and LBO crystals for maximum SHG intensity was performed using a silicon photodetector which generates an electrical pulse with an amplitude proportional to the laser pulse ener.

The 18 mm long KDP I tripler crystal has a 10×10 mm^2 aperture. The KDP optic axis was perpendicular to $\mathbf{E}_{2\omega}$ generated in the KTP II crystal. The THG was a result of the nonlinear interaction of the fundamental wave polarized perpendicular to the

KDP optic axis (having an energy $W_{1\omega}$ equal to half the energy of the remaining fundamental beam after passing through KTP) and SH wave. The third harmonic (TH) electric field $\mathbf{E}_{3\omega}$ and $\mathbf{E}_{2\omega}$ were orthogonally polarized.

The 27 mm long ADP I quadrupler has a 15×15 mm^2 aperture.The ADP optic axis was perpendicular to $E_{2\omega}$. The fourth harmonic (4H) electric field $\mathbf{E}_{4\omega}$ and $\mathbf{E}_{2\omega}$ were orthogonally polarized.

The TH (355 nm) and 4H (266 nm) beams were separated from the fundamental and SH beams with two fused silica prisms P_1, P_2 transparent in UV range. The angular tuning of the KDP and ADP crystals, for maximum TH and 4H intensity, was performed using a pyroelectric detector coupled with an oscilloscope. The pulse energy was measured with a TRG102 calorimeter. The temporal profile of the pulses was visualised on a Tek519 oscilloscope (1 GHz bandwidth) coupled with a fast vacuum photodiode (0.3 ns rise time).

4. Experimental results

The energy of the giant pulse generated by the Nd:YAG laser oscillator was 32 mJ, with 15 ns FWHM pulse width. The waist radius of the TEM_{00} beam, located at the M_2 output mirror [13], was $w_0 \simeq 1.25$ mm, the full divergence angle $\Delta\alpha_f \simeq 0.54$ mrad. The amplifier output pulse energy was 125 mJ. The confocal parameter $b = 2\pi w_0^2/\lambda \simeq 9.2$ m. The nonlinear crystals lay at a distance $d \simeq 0.25$ m from the mirror M_2, $d \ll b/2$, $w_1 \simeq w_0$.

Figure 2 illustrates the sinc^2 curves theoretically deduced from analytical expressions (16) and experimentally measured angular dependence of the normalized harmonics intensity in KTP II, LBO I, KDP I, and ADP I crystals. For KTP II and LBO I the phase matching is in the xy crystallographic plane, the critical rotation is around angle φ, the noncritical rotation is around angle θ. For uniaxial crystals KDP I and ADP I, the critical rotation is around angle θ, the noncritical rotation is around angle $\varphi = 45°$ ($d_{eff} \sim \sin 2\varphi$).

Table 2 summarizes the optical phase matching parameters of the nonlinear crystals (for $w_{1_{KTP}} = 1.25$ mm, $w_{1_{LBO}} = 0.625$ mm, $w_{2_{ADP}} = 0.88$ mm, $w_{1_{KDP}} =$

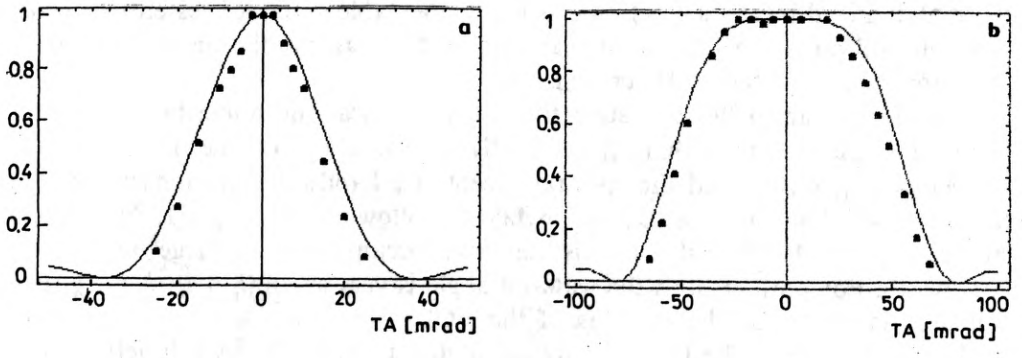

Fig. 2a,b

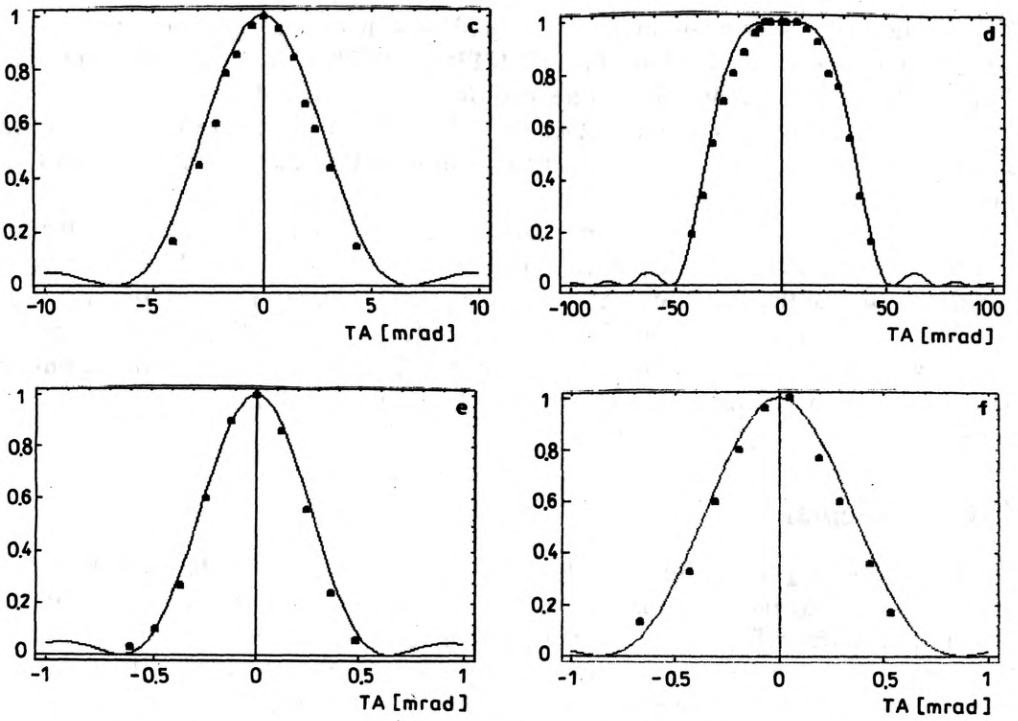

Fig. 2. Measured (data points) and calculated (solid lines) phase matching curves for harmonic generation in different nonlinear crystals as a function of the tuning angle TA. **a** – KTP normalized relative SHG, critical rotation, **b** – KTP normalized relative SHG, noncritical rotation, **c** – LBO normalized relative SHG, critical rotation, **d** – LBO normalized relative SHG, noncritical rotation, **e** – KDP normalized relative THG, **f** – ADP normalized relative 4HG

1.25 mm, $w_{2_{KDP}} = 0.88$ mm) used in our experiments. The acceptance angle and the spectral acceptance bandwidth of the ADP I crystal are comparable with the divergence angle and the bandwidth of the incident 0.532 nm beam. The factor ζ of the conversion efficiency to 4H is reduced by $g_\alpha g_\lambda \simeq 0.7$. We observed high sensitivity of the 4H intensity in ADP with temperature because of the narrow thermal bandwidth (about 1 K). In order to get a stable 4HG, it is essential to work at a constant pulse repetition rate of the incident 2ω laser radiation and to stabilize the temperature of the ADP crystal.

For KTP II and LBO I crystals, the angular critical and noncritical acceptance angles are much wider than the full divergence angle of the incident beam, $(\Delta\theta, \Delta\varphi)_{KTP,LBO} \gg \Delta\alpha_f$, and the spectral acceptance bandwidth is much larger than the Nd:YAG laser line $(\Delta\lambda)_{KTP,LBO} \gg \Delta\lambda_f$. It follows that $g_\alpha g_\lambda \simeq 1$. No thermal stabilization of KTP and LBO is required because of the large temperature bandwidth. For both crystals the walk-off angle is very small ($l_c \ll l_w$, $l_g \simeq l_c$), so we can use Eqs. (11) for the calculus of the ECE.

Figure 3 presents the theoretically calculated ECE to SH as a function of the peak irradiance I_m of the fundamental beam in comparison with the experimentally

Table 2. Phase matching parameters of different nonlinear crystals. $\Delta\theta_c$, $\Delta\varphi_c$ are the calculated acceptance angles. $\Delta\theta_m$, $\Delta\varphi_m$ are measured acceptance angles. $\Delta\lambda$ is the spectral acceptance bandwidth. ΔT is the temperature acceptance bandwidth.

	l_c [mm]	l_w [mm]	l_g [mm]	θ	φ	$\Delta\theta_c$ [mrad]	$\Delta\theta_m$ [mrad]	$\Delta\varphi_c$ [mrad]	$\Delta\varphi_m$ [mrad]	$\Delta\lambda$ [nm]	ΔT [K]
KTP doubler	5	150	4.94	90°	24.5°	107.5	99.4	32.8	30	1.24	56
LBO I doubler	12	86	11.9	90°	10°	70	67.5	6	5.4	3.11	9.15
KDP I tripler	18	30	16.4	47°	45°	0.57	0.54			0.6	14.8
ADP I quadr.	27	69	25.9	80°	45°	0.77	0.72			0.07	1.07

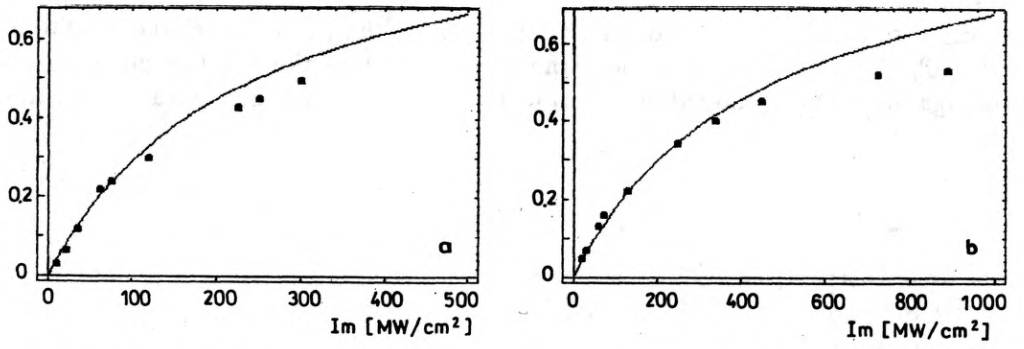

Fig. 3. Measured (data points) and calculated (solid lines) ECE to SH versus peak irradiance I_m of the fundamental Nd:YAG Gaussian beam. **a** – KTP SHG efficiency, **b** – LBO SHG efficiency

measured values for KTP II and LBO I. The maximum ECE measured in the KTP II crystal was 0.48 at $I_m = 300$ MW/cm^2 ($W_\omega = 115$ mJ, $W_{2\omega} = 55$ mJ). The maximum theoretically predicted ECE to SH in a 5 mm long KTP II crystal is about 0.61, under our experimental conditions, restricted by the damage threshold (400 MW/cm^2 at $\tau = 15$ ns). The maximum ECE to SH measured for LBO I crystal was 0.52 at $I_m = 890$ MW/cm^2 ($W_\omega = 87$ mJ, $W_{2\omega} = 45$ mJ). The maximum theoretically predicted ECE in a 12 mm long LBO I is 0.76, under our experimental conditions ($w_{1_{\mathrm{LBO}}} = 0.625$ mm), restricted by the LBO damage threshold (1640 MW/cm^2 at $\tau = 15$ ns).

The maximum measured pulse energy of the TH generated in KDP I was $W_{3\omega} = 15$ mJ ($W_{1\omega} = 30$ mJ, $W_{2\omega} = 55$ mJ). The maximum measured pulse energy of the 4H generated in ADP I was $W_{4\omega} = 19.5$ mJ ($W_{2\omega} = 55$ mJ) corresponding to 17% ECE of the fundamental beam.

5. Conclusions

We have calculated the analytical expressions of the angular acceptance, spectralacceptance, thermal acceptance, and walk-off angle used to evaluate the efficiency of harmonic generation in different nonlinear crystals (KTP II doubler, LBO I doubler, KDP I tripler, ADP I quadrupler). The formulae for the calculus of the walk-off length, interaction length, and SHG efficiency in nonlinear media with non-focused Gaussian laser beams were deduced. The fundamental radiation was generated in a Nd:YAG laser amplifier having a TEM_{00} output pulse energy of 125 mJ with 15 ns FWHM pulse width. We present the measured values of the angular acceptance and ECE to SH in comparison with theoretically calculated values. Analytical expressions show a good agreement with the experimental results.

Appendix

In the case of SHG with a depleted input, under the phase matching conditions ($\Delta k = 0$), the equations describing the collinear interaction of the plane waves propagating along z_1 direction in a transparent medium (at ω, 2ω) can be written [5]:

$$\frac{dA_1}{dz_1} = -\varkappa A_2' A_1,$$
$$\frac{dA_2'}{dz_1} = \frac{1}{2}\varkappa A_1^2 \tag{1A}$$

where $A_2' = iA_2$,

$$A_s = \sqrt{\frac{n_s}{\omega_s}} E_s,$$
$$I_s = \frac{1}{2}\sqrt{\frac{\varepsilon_0}{\mu_0}}\omega_s |A_s|^2 \tag{2A}$$

where $s = 1, 2$, E_s is the electric field, I_s is the irradiance, $\omega_1 = \omega$, $\omega_2 = 2\omega$, $\varkappa$ is given by

$$\varkappa = d_{eff}\sqrt{\frac{2\mu_0\omega^3}{\varepsilon_0 n_1^3}}. \tag{3A}$$

In the slowly varying envelope approximation, the equations of Gaussian waves propagating along z_1 Cartesian axis are:

$$\frac{dA_1}{dz_1} = -\varkappa\gamma(z_1)A_2' A_1,$$
$$\frac{dA_2'}{dz_1} = \frac{1}{2}\varkappa\gamma(z_1)A_1^2 \tag{4A}$$

where $\gamma(z_1)$ is the normalized coupling coefficient between the driving polarization wave Π and the nonlinearly generated electric field E given by

$$\gamma(z_1) = \int_{-\infty}^{\infty} \Pi(x_1,z_1)E(x_1,z_1)dx_1 \int_{-\infty}^{\infty} \Pi(y_1,z_1)E(y_1,z_1)dy_1 \tag{5A}$$

where x_1, y_1 are the Cartesian coordinates of a plane perpendicular to z_1 direction. It follows from Eqs. (4A) that

$$A_2'(l_c) = \frac{1}{\sqrt{2}} A_1(0)\tanh\left[\frac{A_1(0)}{\sqrt{2}}\varkappa\int_0^{l_c}\gamma(z_1)dz_1\right]. \tag{6A}$$

The conversion efficiency to SH of the peak irradiance is

$$\eta_{gp} = \frac{I_m(2\omega)}{I_m} = \frac{2\omega|A_2'(l_c)|^2}{\omega|A_1(0)|^2} = \tanh^2\left[\frac{A_1(0)}{\sqrt{2}}\varkappa\int_0^{l_c}\gamma(z_1)dz_1\right] = \tanh^2[l_g(I_m\zeta)^{1/2}]. \tag{7A}$$

The driving polarization wave at SH for type I phase matching is generated by second order interaction of two *o*-polarized fundamental waves. The spatial profile of the driving polarization has also a Gaussian transverse dependence with a beam radius w_2 given by

$$\frac{1}{w_2^2} = \frac{2}{w_1^2}. \tag{8A}$$

The SH wave assumes the profile of its driving polarization.

For type I phase matching in the LBO crystal the fundamental field is *o*-polarized, the SH field is *e*-polarized, the coupling is given by

$$\gamma(z_1)_{\mathrm{LBO}} = \frac{2}{\pi w_2^2}\int_{-\infty}^{\infty}\exp\left[-\frac{(x_1-\rho z_1)^2}{w_2^2}-\frac{2x_1^2}{w_1^2}\right]dx_1\int_{-\infty}^{\infty}\exp\left[-\frac{y_1^2}{w_2^2}-\frac{2y_1^2}{w_1^2}\right]dy_1$$

$$= \exp\left(-\frac{\pi}{4}\frac{z_1^2}{l_{w_{\mathrm{LBO}}}^2}\right) \tag{9A}$$

where the Poynting vector walk-off angle is confined to the coordinate plane $y_1 = 0$, the walk-off length is

$$l_{w_{\mathrm{LBO}}} = \frac{\sqrt{\pi}}{2}\frac{w_1}{\rho}. \tag{10A}$$

It follows that the interaction length between fundamental and SH beams is

$$l_g = \int_0^{l_c}\exp\left(-\frac{\pi}{4}\frac{z_1^2}{l_w^2}\right)dz_1 = l_w\,\mathrm{erf}\left(\frac{\sqrt{\pi}}{2}\frac{l_c}{l_w}\right). \tag{11A}$$

For ADP I quadrupler the walk-off length of the *e*-polarized 4H wave is

$$l_{w_{ADP}} = \frac{\sqrt{\pi}}{2}\frac{w_2}{\rho} \tag{12A}$$

where w_2 is the beam radius of the incident SH wave.

Neglecting the walk-off of the SH beam generated in the KTP II crystal versus the fundamental beam ($l_{c_{KTP}} \ll w_{1_{KTP}}/\rho_2$), the w_3 radius of the TH beam generated in the KDP I tripler is given by

$$\frac{1}{w_3^2} = \frac{1}{w_2^2} + \frac{1}{w_1^2} = \frac{2}{w_1^2} + \frac{1}{w_1^2} = \frac{3}{w_1^2}. \tag{13A}$$

It follows that the walk-off length of the *e*-polarized TH wave is

$$l_{w_{KDP}} = \sqrt{\frac{\pi}{6}}\frac{w_1}{\rho}. \tag{14A}$$

For type II phase matching in the KTP crystal the fundamental waves are cross polarized, the SH wave is *e*-polarized

$$\gamma(z_1)_{KTP} = \frac{2}{\pi w_2^2}\int_{-\infty}^{\infty} \exp\left[-\frac{(x_1-\rho_2 z_1)^2}{w_2^2} - \frac{x_1^2}{w_1^2} - \frac{(x_1-\rho_1 z_1)^2}{w_1^2}\right] dx_1$$

$$\int_{-\infty}^{\infty} \exp\left[-\frac{y_1^2}{w_2^2} - \frac{2y_1^2}{w_1^2}\right] dy_1 = \exp\left(-\frac{\pi}{4}\frac{z_1^2}{l_{w_{KTP}}^2}\right) \tag{15A}$$

where

$$l_{w_{KTP}} = \frac{\sqrt{\pi}}{2}\frac{w_1}{\sqrt{\rho_2^2 + 0.75\rho_1^2 - \rho_1\rho_2}}. \tag{16A}$$

References

[1] LIN S., SUN Z., WU B., CHEN C., J. Appl. Phys. **67** (1990), 634.
[2] NIKOGOSIAN D. N., Appl. Phys. A **52** (1991), 359.
[3] HEMMATI H., LESH J. R., IEEE J. Quantum Electron. **28** (1992), 1018.
[4] VELSKO S. P., WEBB M., DAVIS L., HUANG C., IEEE J. Quantum Electron. **27** (1991), 2182.
[5] YARIV A., YEH P., *Optical Waves in Crystals*, Wiley, New York 1984.
[6] KOECHNER W., *Solid-State Laser Engineering*, Springer-Verlag, Berlin, Heidelberg, New York 1988.
[7] ZONDY J. J., Opt. Commun. **81** (1991), 427.
[8] MCCARTHY M. J., HANNA D. C., J. Opt. Soc. Am. B **10** (1993), 2180.
[9] ECKARDT R. C., MASUDA H., FAN Y. Y., BYER R. L., IEEE J. Quantum Electron. **26** (1990), 922.
[10] MARSHALL L. R., HAYS A. D., KAZ A., BURNHAM R., IEEE J. Quantum Electron. **28** (1992), 1158.
[11] CRAXTON R. S., JACOBS S. D., RIZZO J. E., BONI R., IEEE J. Quantum Electron. **17** (1981), 1782.
[12] ZERNICKE F., J. Opt. Soc. Am. **54** (1964), 1215; Erratum J. Opt. Soc. Am. **55** (1965), 210.

[13] STRATAN A., FENIC C., DABU R., GROZESCU I. V., MUSCALU L., Proc. SPIE **2461** (1995), 47.
[14] NEBEL A., FALLNICH C., BEIGANG R., WALLENSTEIN R., J. Opt. Soc. Am. B **10** (1993), 2195.

Received June, 10, 1996